










Experimental multiparameter quantum metrology in adaptive regime

Mauro Valeri ^{1,*}, Valeria Cimini ^{1,*}, Simone Piacentini ², Francesco Ceccarelli ², Emanuele Polino ¹, Francesco Hoch,¹ Gabriele Bizzarri,¹ Giacomo Corrielli ², Nicolò Spagnolo ¹, Roberto Osellame ^{2,†} and Fabio Sciarrino ^{1,‡}

¹Dipartimento di Fisica, Sapienza Università di Roma, Piazzale Aldo Moro 5, I-00185 Roma, Italy

²Istituto di Fotonica e Nanotecnologie, Consiglio Nazionale delle Ricerche (IFN-CNR), Piazza Leonardo da Vinci, 32, I-20133 Milano, Italy



(Received 1 September 2022; revised 12 December 2022; accepted 19 December 2022; published 23 February 2023)

Relevant metrological scenarios involve the simultaneous estimation of multiple parameters. The fundamental ingredient to achieve quantum-enhanced performance is based on the use of appropriately tailored quantum probes. However, reaching the ultimate resolution allowed by physical laws requires nontrivial estimation strategies from both a theoretical and a practical point of view. A crucial tool for this purpose is the application of adaptive learning techniques. Indeed, adaptive strategies provide a flexible approach to obtain optimal parameter-independent performance and optimize convergence to the fundamental bounds with a limited amount of resources. Here, we combine on the same platform quantum-enhanced multiparameter estimation attaining the corresponding quantum limit and adaptive techniques. We demonstrate the simultaneous estimation of three optical phases in a programmable integrated photonic circuit, in the limited-resource regime. The obtained results show the possibility of successfully combining different fundamental methodologies towards transition to quantum sensors applications.

DOI: [10.1103/PhysRevResearch.5.013138](https://doi.org/10.1103/PhysRevResearch.5.013138)

I. INTRODUCTION

Quantum correlation has revealed itself to be a fundamental resource in a large variety of fields ranging from computation and communications to metrology and sensing [1–7]. In the latter, the use of quantum probes enables enhanced measurement sensitivity with respect to their classical counterparts. Given this paradigm, several classes of quantum sensors such as atomic clocks and magnetic sensors [8,9] as well as networks of sensors [10–14] have been developed. In several practical scenarios, such as imaging and microscopy, the estimation process generally requires the simultaneous measurement of more than one parameter. This consideration motivated a growing interest in investigating multiparameter quantum estimation, from both a theoretical and an experimental perspective [6,15,16].

Several open challenges still need to be addressed to fully exploit the potential of quantum-enhanced estimation in the multiparameter regime. These open points include the design of appropriate strategies to generate the most suitable probes, depending on the specific set of parameters and on the technological peculiarities of the quantum sensor. Then, the quality of the estimation strategies can be assessed studying the quantum Fisher information (QFI) [17], from which

can be derived the ultimate precision bound consisting in the quantum Cramér-Rao bound (QCRB) [18]. Such a quantity is valid in the asymptotic resource regime and depends on the particular probe state chosen to investigate the process and on its interaction with the parameters of interest. Tighter bounds can be evaluated in different regimes, depending also on the available prior information on parameters [19–22]. After having identified the correct probe, to achieve the ultimate bound, it is necessary to optimize also the adopted measurement strategy. Furthermore, the realization of an actual quantum sensor requires a detailed counting of the number of employed resources. It is then important to optimally allocate them to demonstrate quantum-enhanced sensitivity, independently of the parameter values under investigation. To this aim, a crucial tool is represented by adaptive strategies which are able to optimize the measurement apparatus parameters during the estimation protocols [23].

Multipoint interferometry, which allows multiphase estimation processes to be investigated [24–26], is an especially useful platform to develop such methodologies. Some relevant work has been done in this direction [27,28] in nonadaptive regimes. However, increasing the number of optical modes, and subsequently the number of phases which can be estimated efficiently, requires one to deal with several experimental issues. Indeed, the optimal sensitivity over multiple parameters can be achieved by probing the process with high-dimensional entangled states. The realization of such states is still limited to a small number of modes. To solve scalability issues, integrated photonics represents an optimal solution [29–31], allowing one to implement complex and tunable transformations on the input states. In particular, integrated circuits permit one to easily realize multipoint interferometers with the possibility of handling several embedded phases

*These authors contributed equally to this work.

†roberto.osellame@cnr.it

‡fabio.sciarrino@uniroma1.it

among the different arms. One of the principal strengths of such platforms is the great stability achieved, necessary to implement multiphase estimation protocols. Integrated devices meet almost all the fundamental prerequisites to accomplish quantum-enhanced estimations. Such devices indeed allow one to easily switch the desired input states and the performed measurement schemes, and at the same time they permit a fast tuning of control parameters to implement adaptive protocols.

In this paper, we satisfy simultaneously all the aforementioned requirements in a single experiment. In particular, we report multiparameter estimation of three optical phases, demonstrating experimentally the capability to overcome the optimal separable sensitivity limit, exploiting a two-photon input state with two photons distributed in a four-arm interferometer. Notably, this is done by employing a Bayesian adaptive protocol that allows us to efficiently allocate the number of resources for each estimation, while ensuring an optimized convergence to the ultimate bound in the limited-resource regime. Indeed, the application of real-time adaptive feedbacks enables us to approach such a bound already after only ~ 50 probes. This procedure is shown to provide performance which is independent of the particular value of the unknown parameters. Differently from Refs. [26,28], we implement an adaptive protocol capable of achieving quantum enhancement in a limited-data regime. This kind of protocol has been previously investigated only in the classical regime [32] and for quantum single-parameter estimation [33–35].

Multiparticle input states enable us to perform a multiphase quantum-enhanced estimation which, from a conceptual point of view, represents a paradigmatic test bed for multiparameter estimation protocols in the quantum regime. Finally, we compare our results with the ones achievable by probing the system with a sequence of optimal classical probe states, demonstrating an enhancement in the simultaneous estimation of the three phases, surpassing the classical limit and saturating the QCRB.

A. Multiparameter quantum metrology: Multiphase estimation

A multiparameter approach to quantum metrology has proven to be beneficial in different scenarios where the simultaneous estimation of multiple parameters can provide better precision than estimating them individually by using the same amount of resources [15,16,19,24,25,36]. Note that different strategies and paradigms have been recently considered to quantify the corresponding achievable limits [37,38]. Furthermore, in an actual experiment, even if the parameter of interest is a single one, the estimation process unavoidably involves other parameters, linked to noise, which have to be estimated simultaneously to provide an unbiased estimation [39,40]. While in the single-parameter scenario the QCRB can in principle be always saturated choosing appropriate measurement schemes, an additional problem arises in the multiparameter case. Here, the saturability of the bound is not always guaranteed [41,42]. It is of particular interest to identify, within such a framework, quantum resources able to obtain a sensitivity advantage versus classical strategies. The ultimate achievable bound is indeed related to the estimation of the vector $\boldsymbol{\varphi} = (\varphi_1, \varphi_2, \dots, \varphi_d)$ of d parameters becoming

an inequality on their covariance matrix:

$$\Sigma(\boldsymbol{\varphi}) \geq \frac{\mathcal{F}_C^{-1}(\boldsymbol{\varphi})}{M} \geq \frac{\mathcal{F}_Q^{-1}(\boldsymbol{\varphi})}{M}, \quad (1)$$

where M is the number of independent probes employed and the covariance matrix is given by

$$\Sigma(\boldsymbol{\varphi})_{ij} = \sum_{\mathbf{x}} [\hat{\varphi}(\mathbf{x}) - \varphi]_i [\hat{\varphi}(\mathbf{x}) - \varphi]_j P(\mathbf{x}|\boldsymbol{\varphi}). \quad (2)$$

Here, $i, j = 1, \dots, d$, $\hat{\boldsymbol{\varphi}}$ is the list of estimators of $\boldsymbol{\varphi}$, \mathbf{x} are the possible outcomes, and $P(\mathbf{x}|\boldsymbol{\varphi})$ is the likelihood of the estimation process. In the inequalities, \mathcal{F}_C is the Fisher information (FI) matrix defined as $\mathcal{F}_C(\boldsymbol{\varphi})_{ij} = \sum_{\mathbf{x}} [\frac{1}{P(\mathbf{x}|\boldsymbol{\varphi})} \frac{\partial P(\mathbf{x}|\boldsymbol{\varphi})}{\partial \varphi_i} \frac{\partial P(\mathbf{x}|\boldsymbol{\varphi})}{\partial \varphi_j}]$, while $\mathcal{F}_Q(\boldsymbol{\varphi})$ is the quantum Fisher information (QFI) matrix. The first inequality is referred to as the Cramér-Rao bound (CRB), while the second inequality, i.e., QCRB, in the multiparameter scenario is fulfilled only if the collective saturation of the bound for all the parameters is simultaneously verified [43]. Therefore of particular interest are those situations where the optimal measurement schemes for each parameter are compatible and consequently the right hand of the inequality (1) becomes an equality, making the CRB equal to the QCRB. Such bounds are relative to the frequentist approach [44] where the parameter is approximated with the estimator that usually coincides with the one maximizing the likelihood of the measurement results. The sensitivity of the multiparameter estimation can be obtained by computing the trace of the covariance matrix, which is then compared with the trace of the FI and of the QFI. Note that this is not the only possible choice for the definition of sensitivity. Indeed, different figures of merit can be used, such as sums of FI terms with general weights [45].

The saturation of the QCRB is verified asymptotically; therefore, in a real scenario where only a limited amount of resources is available, it is important to optimize them at each step in order to ensure the convergence. The optimization of the resources can be implemented through adaptive strategies which indeed ensure a faster convergence to the ultimate bound. Adaptive Bayesian estimation protocols are usually employed to accomplish such tasks [23,32,46–52], where at each step the posterior distribution is updated depending on the settings of some control parameters. Although the aforementioned bounds are not computed for Bayesian estimation, in the limit of a large number of repeated measurements the frequentist and the Bayesian methods agree; therefore the QCRB can still be employed as a reference for Bayesian settings in the asymptotic regime.

One of the most investigated frameworks for studying multiparameter estimation is optical interferometry, where the unknown parameters are mapped in the different phase shifts between the arms of an interferometer with respect to a reference [24–28,32,37,51,53–58]. The quantum estimation of phases is of paramount importance for different applications: Apart from direct use in sensing such as biological imaging [59–62], it can be employed also in tasks such as quantum communication [63], simulation [64], and even gravitational wave detection [65].

Lastly, and importantly, multiphase estimation is a paradigmatic scenario representing a fundamental test bed for general multiparameter estimation protocols. In this context, a probe

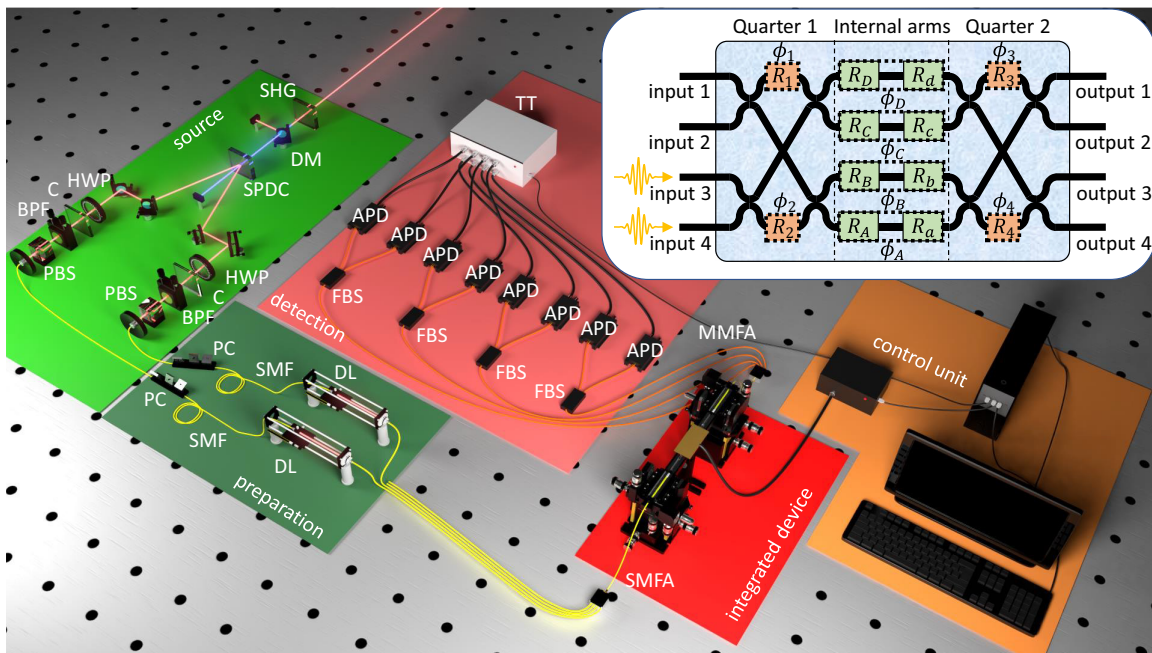


FIG. 1. Full experimental setup employed for multiphase estimation experiments on chip. (i) Source. Two-photon states are generated via parametric down-conversion in a β -barium borate (BBO) crystal. (ii) Preparation. Photons are made indistinguishable in time via delay lines, and in the polarization degree of freedom via fiber polarization controller. (iii) Integrated device. Photons are injected in the integrated interferometer, and collected at the output, via fiber arrays. (iv) Detection. Two-photon events are collected via a probabilistic photon-counting scheme. (v) Control unit. Measurement outcomes are processed by the control unit and are used to drive the thermal shifter operation. Inset: Scheme of the integrated circuit. Each thermal shifter R_i is able to control a specific optical phase of the device. In particular, with regard to the internal arms of the interferometer, we identify the three independent internal phase shifts $(\varphi_A, \varphi_B, \varphi_D) := (\phi_A - \phi_C, \phi_B - \phi_C, \phi_D - \phi_C)$ by setting C as the reference arm. Instead, ϕ_1, ϕ_2, ϕ_3 , and ϕ_4 define the equivalence class of each quarter transformation. SHG, second-harmonic generation; DM, dichroic mirror; SPDC, spontaneous parametric down-conversion; HWP, half-wave plate; C, walk-off compensation; BPF, bandpass filter; PBS, polarizing beamsplitter; PC, polarization compensation; SMF, single-mode fiber; DL, delay line; SMFA, single-mode fiber array; MMFA, multimode fiber array; FBS, fiber beamsplitter; APD, avalanche photodiode; TT, time tagger.

$|\Psi_0\rangle$, prepared by a suitable operation in the space of $d + 1$ modes, interacts with the phase shifts through the unitary evolution: $|\Psi_\varphi\rangle = e^{i(\sum_{i=1}^d n_i \varphi_i)} |\Psi_0\rangle$, where n_i is the generator of the phase φ_i along the mode i , i.e., the photon number operator for that mode. Since such generators commute, $[n_i, n_j] = 0 \forall i, j$, the QFI matrix $\mathcal{F}_Q(\varphi)_{ij} = 4[\langle n_i n_j \rangle - \langle n_i \rangle \langle n_j \rangle]$, where the average $\langle \cdot \rangle$ is over $|\Psi_\varphi\rangle$ and the probe states are assumed to be pure [6]. Finally, after a final transformation, the state is measured and an estimator provides the estimation of the unknown phases. It has been demonstrated that the optimal quantum probe state, together with the optimal measurement, can achieve quantum-enhanced performance with also an advantage of order $O(d)$ over the best quantum precision for the phases estimated separately [25]. Note that the improvement $O(d)$ achieved by the simultaneous estimation is reduced to a constant if the resource count is chosen differently [37].

Particular interest needs to be devoted to identify those configurations, i.e., the number of optical modes constituting the arms of the multipoint interferometer and the possible input states, which allow us to saturate the ultimate bound of precision [24]. These configurations demonstrate enhanced performance compared with the use of classical probe states. In particular, states having a coherent superposition of M photons in one mode and none in the others, allowing the simultaneous estimation of multiple phases, achieve advan-

taged performance compared with any classical probe states. The need to control the input states, as well as the performed measurements, and to configure some control parameters to implement adaptive protocols requires a versatile and programmable platform. All these conditions are attained by integrated photonics, which represents a promising platform for quantum sensing and metrology studies and applications [30].

II. RESULTS

A. Integrated multipoint interferometer for quantum sensing

Our platform consists of an actively tunable integrated four-arm interferometer realized through femtosecond laser waveguide writing in glass [31,66]. In particular, the device is composed of two cascaded quarters, which are 4×4 optical elements that split equally the optical power at all its input ports across all output ports. Each quarter is composed of four directional couplers arranged in a two-layer configuration and a three-dimensional waveguide crossing, as depicted in Fig. 1. Moreover, each quarter is equipped with two thermal phase shifters (R_1, R_2, R_3, R_4), which allow us to actively control the internal optical phase between the directional coupler layers ($\phi_1, \phi_2, \phi_3, \phi_4$) and select a specific equivalence class of the quarter transformations [67]. Between the two quarters, the interferometric region is composed of four straight

waveguide segments whose optical phases $\phi_A, \phi_B, \phi_C, \phi_D$ can be controlled by means of eight thermal phase shifters (R_a, R_b, R_c, R_d ; and R_A, R_B, R_C, R_D). The overall length of the device is 3.6 cm. All thermal shifters have been fabricated by femtosecond laser micromachining and include laser-ablated isolation trenches around each microheater [68]. This configuration allows us to both reduce the power consumption (a 2π phase shift on a single resistor is obtained by dissipating less than 25 mW of electrical power) and greatly reduce the thermal cross talk between adjacent shifters. More details regarding the circuit geometry, the waveguide inscription, the thermal shifter fabrication processes, and the thermal shifter performance are provided in Note 1 of the Supplemental Material [69]. Finally, two four-channel single-mode fiber arrays have been glued at the interferometer input and output facets, with average fiber-to-fiber total insertion losses (from the connector of the input fiber to the connectors of the output fiber array) of 2.5 dB (insertion loss of the bare device before pigtailling of 1.5 dB). Hence the overall efficiency of the whole apparatus from the source to the detection is $\eta_{\text{overall}} \sim 3\text{--}5\%$.

On the basis of the presented scheme, the transformation performed by the phase shifters fabricated on the internal arms of the interferometer reads

$$U_\phi = \begin{bmatrix} e^{i\phi_D} & 0 & 0 & 0 \\ 0 & e^{i\phi_C} & 0 & 0 \\ 0 & 0 & e^{i\phi_B} & 0 \\ 0 & 0 & 0 & e^{i\phi_A} \end{bmatrix}, \quad (3)$$

while the relation linking the dissipated power ω to the inserted phase shift can then be approximated by

$$\varphi_i = \sum_j (\alpha_{ij}\omega_j + \alpha_{ij}^{(2)}\omega_i\omega_j) + \varphi_{0i}, \quad (4)$$

where φ_0 is the zero-current phase shift, while α and $\alpha^{(2)}$ are the linear and quadratic response coefficients associated with the phase shift φ , respectively. In particular, in our device, 12 thermo-optic phase shifters can be suitably controlled. The interferometer is able to perform the simultaneous estimation of three independent phase shifts φ between three arms and a reference one. In the following, we choose C as the reference arm, thus considering $(\varphi_A, \varphi_B, \varphi_D) \equiv (\phi_A - \phi_C, \phi_B - \phi_C, \phi_D - \phi_C)$ as the triple phases to be estimated. The transformation induced by the actual device will also depend on the effective transmittivities and reflectivities of the eight directional couplers.

We start by theoretically studying the operation and the bounds relative to the ideal device, i.e., when the reflectivities and transmittivities of all the directional couplers are equal to the nominal value of $\frac{1}{2}$. The QFI depends only on the prepared probe state; therefore it is a function of the input modes of the injected photons and of the phases ϕ_1 and ϕ_2 of the first quarter, whose transformation is given by

$$U_Q = \frac{1}{2} \begin{bmatrix} e^{i\phi_2} & ie^{i\phi_2} & i & -1 \\ ie^{i\phi_2} & -e^{i\phi_2} & 1 & i \\ i & 1 & -e^{i\phi_1} & ie^{i\phi_1} \\ -1 & i & ie^{i\phi_1} & e^{i\phi_1} \end{bmatrix}. \quad (5)$$

However, depending on the specific input, the dependence on these two phases can vanish. More specifically, this condition

is verified when injecting two photons either in the first two modes ($|1100\rangle$) or in the last two ($|0011\rangle$). Such a choice allows us to generate, after the first quarter, the multiphoton entangled input state:

$$|\psi_0\rangle = \frac{i}{2\sqrt{2}}(|2000\rangle - |0200\rangle + e^{-2i\phi_1}|0020\rangle - e^{-2i\phi_1}|0002\rangle) - \frac{1}{2}(|1100\rangle + e^{-2i\phi_1}|0011\rangle). \quad (6)$$

For our device, the use of two-photon quantum probes ensures that we approach the ultimate asymptotic quantum limit for the three-phase estimation represented by the relative QCRB, which is $2.5/M$. The computed bound represents the ultimate quantum limit achievable in the estimation precision for the considered input. The overall amount of resources is $2M$ single photons, thus taking into account the computation of such a bound for M independent two-photon states. More specifically, we count as resources only the effective detected photon pairs, thus working in a postselection configuration.

The optimality of the full scheme is therefore demonstrated when the CRB, obtained after the measurement process is also considered, reaches the QCRB. Therefore, when studying the CRB, the characteristics of the second quarter must also be considered in the model. The state generated at the output after injecting into the device two photons in the third and fourth inputs is a coherent superposition of two photons in the four output modes of the device:

$$|\psi\rangle_{\text{out}} = a_{11}|2000\rangle + a_{22}|0200\rangle + a_{33}|0020\rangle + a_{44}|0002\rangle + a_{12}|1100\rangle + a_{13}|1010\rangle + a_{14}|1001\rangle + a_{23}|0110\rangle + a_{24}|0101\rangle + a_{34}|0011\rangle, \quad (7)$$

with $a_{11} = a_{22}$, $a_{33} = a_{44}$, $a_{13} = a_{24}$, and $a_{23} = a_{14}$, where all the coefficients now depend on the parameters imposed by U_Q transformation and on the particular settings of ϕ_1 , ϕ_2 , ϕ_3 , and ϕ_4 . The CRB, given such a state, can indeed saturate the ultimate limit of $2.5/M$, satisfying the general necessary conditions for the saturation of QCRB of multiphase estimation in interferometric setups [27]. It is fundamental to notice that indistinguishability between the two input photons is a necessary condition to reach such a bound. The minimum of the CRB in the scenario of indistinguishable photons ensures the saturation of the QCRB and the achievement of a quantum-enhanced estimation over three parameters. Indeed, the use of completely distinguishable photons allows us to achieve a minimum equal to 3 (see Note 2 of the Supplemental Material for details).

To demonstrate the capability of reaching an estimation enhancement, we compare our result also with the optimal estimation obtained through single-photon states [25]. In order to make a fair comparison, it is important to consider the same number of photons for classical strategies. In this case, the trace of the inverse Fisher information matrix is 5.6 for a single photon prepared in the optimal state. Therefore preparation of two independent photons in such a state corresponds to a value of 2.8 for the trace of the inverse Fisher information matrix. Hence a strategy employing $2M$ independent optimal single-photon states is associated with an achievable bound of $\text{QCRB} = 2.8/M$. Therefore the saturation of $2.5/M$

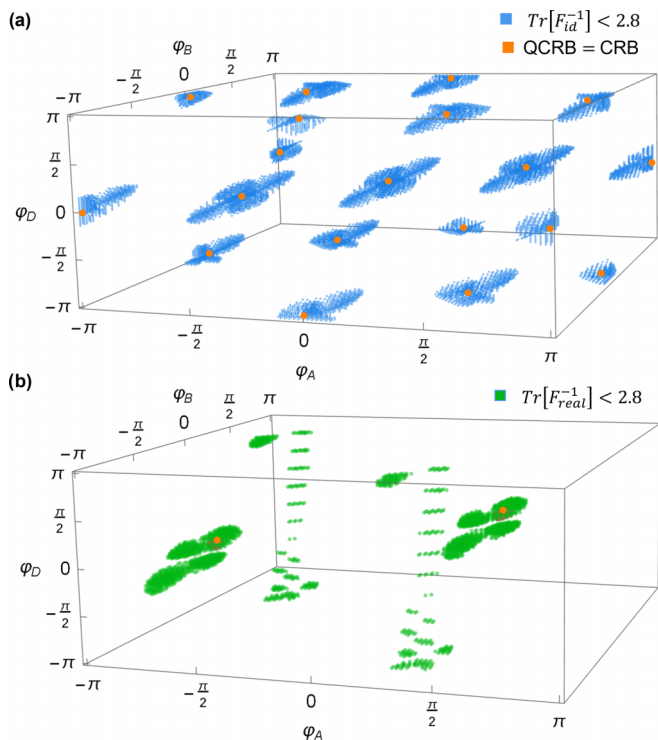


FIG. 2. Cramér-Rao bound regions. Points corresponding to a value of the CRB $< 2.8/M$. The orange points correspond to the minimum where the QCRB is saturated. (a) Bound relative to the ideal device. (b) Bound for the real device whose minimum is $2.53/M$.

demonstrates quantum-enhanced measurement sensitivity reachable with indistinguishable two-photon states compared with any sequence of classical single-photon probes and independent measurement, even including the optimal single-photon state.

The parameter (phase) regions showing such an advantage where the achieved CRB, for the ideal device, is lower than 2.8 are limited and are reported in Fig. 2(a). However, thanks to the implementation of an adaptive protocol we are able to demonstrate the sensitivity enhancement independently of the values of the estimated triplet of optical phase shifts in the limited-resource regime.

B. Experimental saturation of the ultimate quantum Cramér-Rao bound

In order to investigate the actual capabilities of the employed device with two-photon input states, it is necessary to reconstruct its likelihood function through a calibration procedure (see Note 3 of the Supplemental Material for details). This step is necessary to derive the achievable CRB with the actual device.

We reconstruct the ten two-photon output probabilities by fitting the measured data for different values of voltages applied to the resistors of the device. In particular, we collect measurements studying the device response as a function of the power dissipated on the three thermal shifters, i.e., R_a, R_b, R_d , allowing the complete tuning of the internal phases. In this way, using Eq. (4), we can model also the effect that the voltage applied on a certain resistor has on

the other arms of the device, retrieving all the different cross talks among the resistors. More specifically, we measure the coincidence events registered at the output of the integrated circuit by dissipating through each selected resistor ten different power values, which are equally spaced over the allowed range. More technical details regarding the characterization data can be found in Note 3 of the Supplemental Material.

Finally, the output probabilities reconstructed from experimental data can be used to compute the FI matrix and to retrieve the experimental CRB. In Fig. 2(b) we report the regions showing a bound lower than the minimum one achievable with the best classical states for such measurement. To highlight the regions of minimum uncertainty, we report three cuts of the inverse of the trace of the FI in Fig. 3, where the explicit two-variable function is plotted. From these plots it is evident that the estimation uncertainty is highly related to the particular value of the triplet of phases under study. In order to perform the estimation in the point of minimum uncertainty independently from the particular value of the triplet investigated, it is therefore necessary to implement an adaptive strategy which sets the device always in its more informative point. For the actual device, considering all the experimental imperfections, the minimum which corresponds to the achievable bound is $2.53/M$, and it is achieved in two different points of the space [see Fig. 2(b)]. Note that this bound has been obtained considering all the main sources of imperfections affecting the experimental setup. More specifically, we consider the nonunitary indistinguishability of the two input photons and deviations from the ideal behavior of the transformations performed by the optical elements in the integrated device, including transmittivities of the directional couplers and different detection efficiencies. This value is very close to the ideal one of $2.5/M$, and it is still below the critical threshold of 2.8. With our device we demonstrate quantum enhancement in the simultaneous estimation of three optical phases, experimentally approaching the QCRB in a postselected configuration.

C. Comparison with the sequential bound

In a general scenario, we can study the sensitivity performance obtained when estimating a linear combination of the parameters under study. Distributed sensing [10–14] represents indeed a field that has been increasingly investigated lately. However, instead of looking at any generic combination of parameters $\mathbf{v} \cdot \boldsymbol{\varphi} = \sum_{i=1}^d v_i \varphi_i$, here, following Ref. [45], we can study the achieved performance over the optimal combination of phases to show the quantum-enhanced sensitivity. Therefore we compare for our setup the sensitivities reached with the simultaneous multiparameter estimation with respect to sequential strategies where the different parameters are all estimated independently. In particular, the optimal vector \mathbf{v} for our setup is the eigenvector of the QFI matrix associated with the largest eigenvalue f_{\max} , i.e., $\mathbf{v}_{\max} = (1/2, 1/2, -1/\sqrt{2})$. It follows that the optimal linear combination of optical phases that we can estimate is $(\phi_A - \phi_D)/2 + (\phi_B - \phi_D)/2 - (\phi_C - \phi_D)/\sqrt{2}$. The study of this figure of merit allows us to consider also the off-diagonal terms of the QFI that in general depend on mode entanglement in the probe state. It is then possible to compute the sensitivity bound on the estimate of

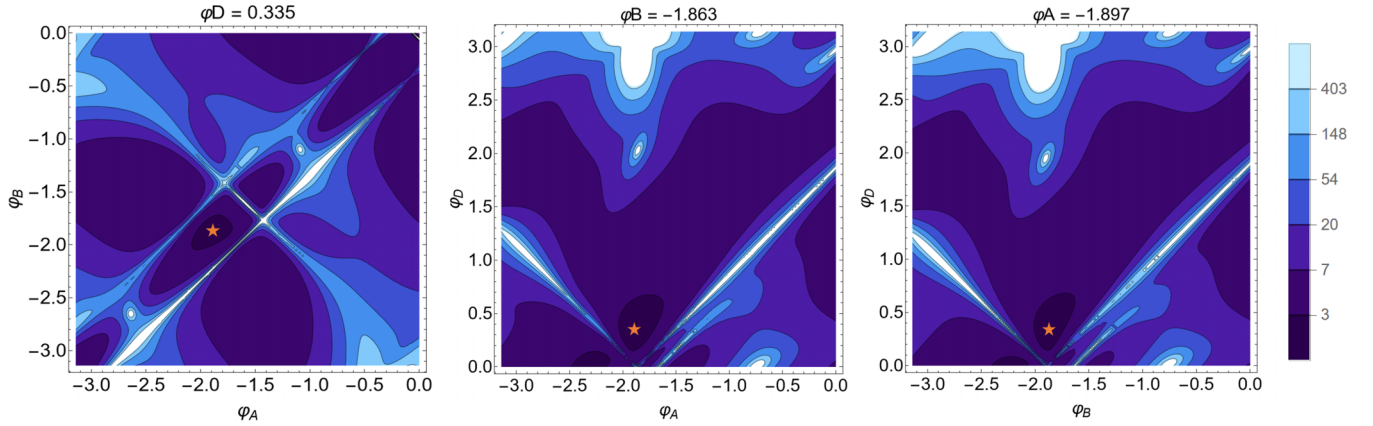


FIG. 3. Slices of the Fisher information matrix. Three cuts of $\text{Tr}[F^{-1}]$ obtained fixing, in the left, middle, and right panels, the values of φ_D , φ_B , and φ_A , respectively. The plots show the sensitivity of different regions of the parameter space. The orange star represents the minimum of the variance where the CRB is equal to $2.53/M$, which indeed coincides with the orange point in Fig. 2(b). The color legend has been chosen to be logarithmic in order to highlight the regions associated with the minimum uncertainty.

the linear combination, achieved when using the employed entangled input states, which is given in Ref. [45], and the result is

$$\Delta^2(\mathbf{v}_{\max} \cdot \boldsymbol{\varphi}) = \mathbf{v}_{\max} \mathcal{F}_{\mathcal{Q}} \mathbf{v}_{\max}^T = 0.292. \quad (8)$$

The comparison can be done with the optimal separable strategy achieved using coherent states with an average number of photons $\langle \bar{n} \rangle = 2$ to estimate sequentially three optical phases embedded in a network of Mach-Zehnder interferometers. In such a setting, the QCRB is

$$\Delta^2(\mathbf{v}_{\max} \cdot \boldsymbol{\varphi})_{\text{seq}} = \sum_{i=1}^3 \frac{v_i^2}{\mathcal{F}_i}. \quad (9)$$

Here, \mathcal{F}_i is the single-parameter QFI for coherent states injected into a Mach-Zehnder interferometer, i.e., $\mathcal{F}_i = \bar{n}_i$ [70]. By numerical optimization, we obtain the minimum of $\Delta^2(\mathbf{v}_{\max} \cdot \boldsymbol{\varphi})_{\text{seq}} = 1.45$, corresponding to the bound achievable with sequential classical measurements. Consequently, a sensitivity in the estimation of the optimal linear combination below this separable bound is a demonstration of the enhancement achieved using entangled probes [45].

D. Adaptive three-phase estimation

Finally, we study the performance achieved when implementing adaptive strategies, able to set the device in the optimal working point for the estimation [23,32,46–48]. This optimization can be done before each probe, and it is independent of the specific unknown values. It is based on controlling additional parameters, used as feedbacks during the estimation cycle [Fig. 4(a)]. Adaptive techniques are used when the number of resources is limited or to solve estimation ambiguities related to the output probability of the system. The capability of asymptotic saturation of lower bounds is not sufficient when an optimal estimation in a few probes is required. Moreover, the computation of which optimal feedbacks have to be applied is in general nontrivial, especially for increasing complexity of the system. For this reason, machine learning techniques are often adopted, able to tackle this hard

computational task and in general to enhance sensing protocols [6,52,71–76].

Here, we employ a Bayesian framework (see the Supplemental Material for details) for the adaptive protocol, which represents a powerful tool for multiphase estimation [50,51]. In particular, we use the Bayesian multiparameter estimation protocol employed in Refs. [32,50,77]. Simultaneous adaptive two-phase estimation experiments have been demonstrated without quantum enhancement, injecting a three-mode interferometer with single-photon states [32]. Thus we select such an approach for our multiphase estimation problem demonstrating the saturation of the ultimate precision bounds.

The realization of adaptive multiphase estimation requires the identification of unknown and control parameters. The structure of our platform allows us to handle independently two layers of internal phases by simply acting on different resistors: the phases to be estimated $\boldsymbol{\varphi}^{(X)}$ and the phases to be tuned for adaptive estimation $\boldsymbol{\varphi}^{(C)}$, such that $\boldsymbol{\varphi} = \boldsymbol{\varphi}^{(X)} + \boldsymbol{\varphi}^{(C)}$. In our case, the triplet of unknown parameters $\boldsymbol{\varphi}^{(X)}$ is set using the thermal shifters R_A, R_B, R_D , while the control parameters $\boldsymbol{\varphi}^{(C)}$ are tuned using R_a, R_b, R_d . To easily achieve adequate control for each estimate, the calibration of resistors R_a, R_b, R_d can be repeated for each selected triplet R_A, R_B, R_D . This method guarantees also a more precise calibration of the specific working point of the device.

The algorithm is based on a sequential Monte Carlo (SMC) technique, and it is discussed in detail in the Supplemental Material. The SMC guarantees a high level of performance in computing integrals—replaced by sums—also when the dimensions of the space increase. The quality of the approximation can be improved by adding further particles, at the cost of a more expensive computation. Then the algorithm allows the computation of the control parameters to be applied during the adaptive estimation. Such optimal values are those which maximize the expected overall variance after measurement of the subsequent probe. Here, the expectation value is computed using the SMC approach. In order to identify appropriate values of the algorithm parameters for the experiment, we simulated adaptive multiphase estimations for different configurations of such parameters. A set of phase triplets $\{\boldsymbol{\varphi}^{(X)}\}$

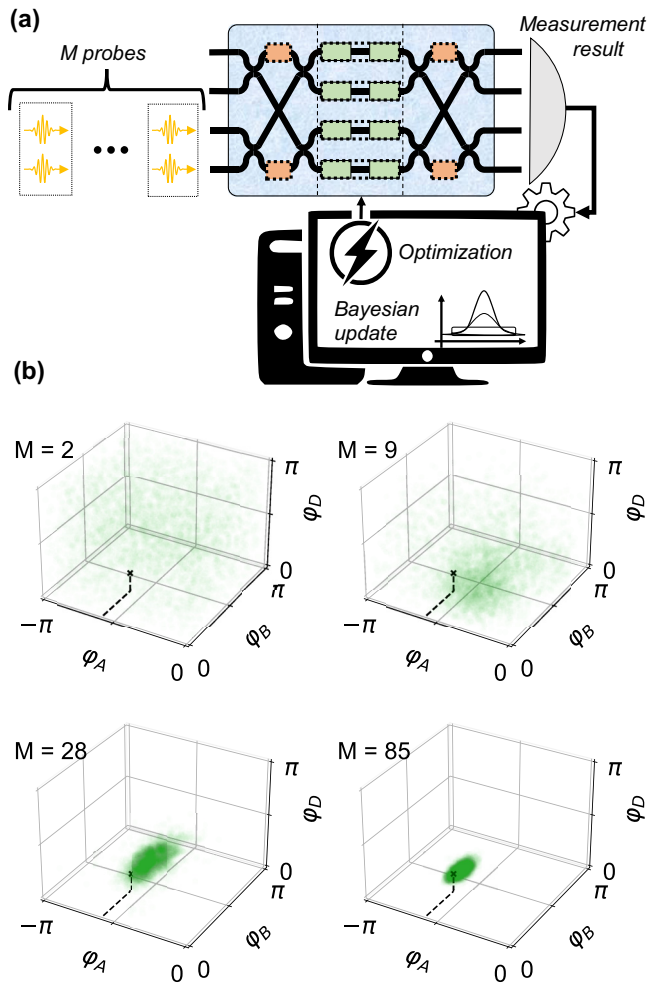


FIG. 4. Adaptive estimation and control feedbacks. Example of adaptive multiparameter Bayesian learning by injecting a series of M probes into the device. (a) After each measurement result, the algorithm computes the best control parameters, i.e., a set of currents to apply for optimizing the estimation efficiency of the next probe. At the same time, each measured probe updates the knowledge of the parameters according to Bayes' rule, concentrating the probability distribution around the true values. (b) Evolution of posterior knowledge (green cloud) after sending 2, 9, 28, and 85 probes to estimate the three phases $(\varphi_A^{(X)}, \varphi_B^{(X)}, \varphi_D^{(X)}) = (-1.82, 1, 0.54)$ simultaneously. The distribution converges rapidly around the true values of the triple phases (black cross).

is uniformly selected in $[0, 2\pi] \times [0, 2\pi] \times [0, 2\pi]$ and estimated by a series of two-photon states. The estimation of each triplet is repeated 30 times. A single experiment of adaptive three-phase estimation is reported in Fig. 4(b), by showing how the updated posterior distribution converges to the true value after sending 2, 9, 28, and 85 probes. The output probability distribution of our device, given the considered entangled input state, can estimate unambiguously each of the three phases in a π range. For this reason, we set the *a priori* Bayesian distribution equal to a uniform distribution with a π width. Note that, by repeating the estimation procedure several times, we obtain the mean of the Bayesian posterior distribution, from which we retrieve the achieved sensitivity

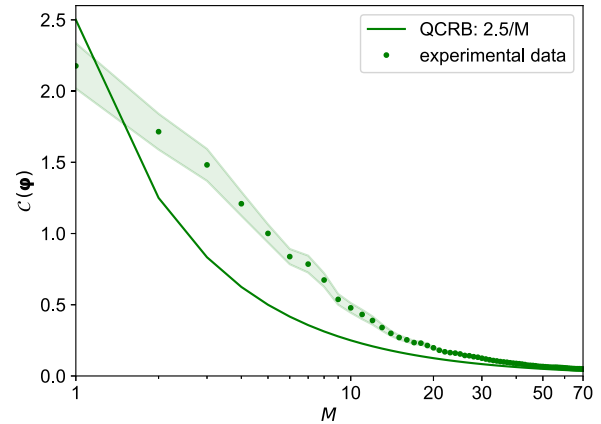


FIG. 5. Experimental adaptive three-phase estimation. Quadratic loss $\mathcal{C}(\varphi)$ is plotted as a function of the number M of injected two-photon input states $|0011\rangle$. Green dots show the performance averaged on 12 different triple phases, estimated using the online Bayesian adaptive technique described in the text. The experiment for each phase triplet is repeated 30 times, and the final performance is characterized by the mean estimator; the shaded green area is the one-standard-deviation region. The solid line is the ultimate precision bound, i.e., the QCRB ($2.5/M$) for the ideal device when injected with indistinguishable photons.

for all the performed repetitions, allowing us to compare our results with the bounds of the frequentist scenario.

The accuracy of the estimation can be computed looking at different figures of merit. We start investigating one that was commonly employed in the first studies of multiphase estimation [25] by firstly considering a figure of merit that takes into account the trace of the covariance matrix. Then, we generalize the discussion considering also the off-diagonal terms of the covariance matrix, when demonstrating quantum-enhanced sensitivity for the estimate of a linear combination of the considered parameters. The covariance of the posterior distribution $\Sigma(\hat{\varphi})$ represents the confidence interval of the estimate and thus the actual error of the quantum sensor employed. In parallel, the quadratic loss distance $\mathcal{C}(\varphi)$, between the estimated parameters and their true values, provides a reliable evaluation of both the estimation uncertainty and the presence of possible biases. Such quantities are obtained as follows: $\mathcal{C}(\varphi) = (\varphi - \hat{\varphi})^T (\varphi - \hat{\varphi})$ and $\Sigma(\hat{\varphi}) = \int (\varphi - \hat{\varphi})^2 p(\varphi|d) d\varphi$, where $p(\varphi|d)$ represents the posterior probability which is updated through the Bayesian procedure after each measurement result d has been registered. In the asymptotic regime the average of both the covariance and the quadratic loss $\mathcal{C}(\varphi)$ must saturate the CRB. Conversely, this does not represent a stringent bound in the low-number-of-probes regime due to the *a priori* knowledge retained on the parameter values as discussed in more detail in Ref. [20]. Here, we employ the adaptive technique in order to approach the ultimate precision bound with the minimum number of probes, reporting the experimentally attained quadratic loss function averaged over 12 different triplets of phases. As shown in Fig. 5 we are able to reach a performance close to the asymptotic limit already after sending around 50 probes.

Finally, we also use the adaptive approach to study the estimation of the optimal linear combination of the three

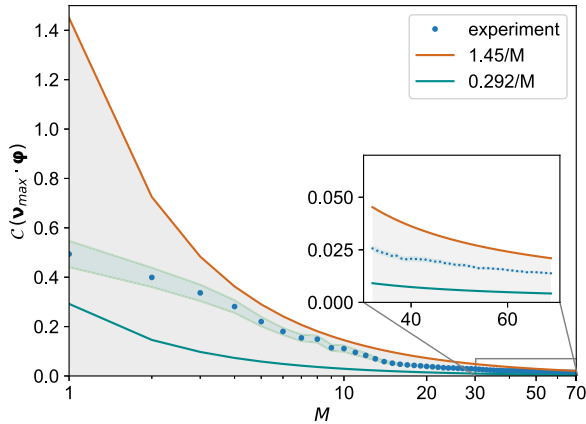


FIG. 6. Experimental adaptive performance. Estimation performance as a function of the employed resources is reported in terms of $C(\mathbf{v}_{\max}, \boldsymbol{\varphi})$. The experimental data with the relative standard deviation (shaded blue region) are averaged over 12 phases estimated 30 independent times. For comparison, both the separable (orange line) and parallel (cyan line) bounds are provided. The shaded gray area represents the region showing enhanced sensitivity compared with sequential strategies. The inset shows a zoom of the behavior for a number of two-photon probes in the range $M = 30\text{--}70$.

parameters discussed in the previous section. The results of the experimental estimates are reported in Fig. 6. Here, we manage to outperform classical separable strategies, by showing that the average over multiple repetitions of the estimation protocol performed on different triplets of phases is found to be below the sequential bound. Note that, in this paper, we demonstrate experimentally the violation of the sequential bound, assuring the convenience of adopting parallel strategies in multiphase estimation problems.

III. DISCUSSION

In this paper we have addressed some of the most relevant open issues of multiphase estimation, satisfying simultaneously all the relevant requirements of practical multiparameter quantum metrology in a postselected configuration. We demonstrate the saturation of the ultimate precision bound, i.e., the QCRB employing multiphoton entangled states. We experimentally prove the enhancement achieved using entangled probes over optimal separable estimation strategies when estimating an optimal linear combination of the investigated parameters [45]. Furthermore, to grant the optimal sensitivity in the practical limited-resource regime, we implement a Bayesian adaptive multiparameter technique, which requires us to operate on a suitably programmable platform applying real-time feedbacks. We performed our experiment through a versatile setup by means of a state-of-the-art integrated circuit with low insertion losses, low power dissipation, and high reliability of the thermal phase shifters, all characteristics that will allow the number of spatial modes and the complexity of the devices to be further scaled up in the future.

We characterized the integrated circuit using two-photon quantum states and then reconstructing the likelihood function of the device operation. From the collected output statistics,

we were able to retrieve the FI matrix of the apparatus, demonstrating the saturation of the QCRB on sensitivity. Then, we exploited the circuit to perform an optimal Bayesian adaptive protocol that allowed us to approach the quantum limits after only ~ 50 resources. Notably, the obtained precision is higher than the one achievable by the best sequential classical strategy estimating the three phases independently.

The results shown here represent an important step towards the achievement of practical quantum metrology (as shown in a table in the Supplemental Material). In particular, in this paper we extend multiparameter adaptive strategies to the quantum realm, accomplishing this task within a versatile and scalable integrated device, approaching ultimate quantum bounds when estimating simultaneously three parameters and overcoming recently introduced sequential bounds.

The demonstrated approach will be the test bed for general quantum multiparameter estimation protocols [52], and it will empower different applications, from biological sensing [78–81] to improving strategies for error compensation in quantum communication protocols working in the single-photon regime [82]. Furthermore, protocols for the synchronization of networks of sensors [83,84] can also benefit from the demonstrated technique. Finally, our findings can be applied even in tasks of quantum computation and simulation whose subroutines often rely on quantum phase estimation algorithms [64,85,86]. To reach a fully scalable and convenient quantum sensor, two other issues have to be addressed, simultaneously with those closed here. The first one is the scaling of quantum resources: In order to achieve quantum scalings with a large number of resources [87], either different kinds of encoding [88] or more efficient sources such as quantum dots [89] are required. Finally, the unconditional quantum advantage can be claimed if classical limits are overcome even when all the generated resources, including loss and noise mechanisms, are taken into account [10,90]. The most relevant sources of losses lie in the generation and collection of photons. A possible solution to the former is represented by integrated sources [91,92] that can be directly interfaced with integrated interferometers. For the detection efficiency, a possible solution is the use of superconductive single-photon detectors with near-unity efficiency [93].

ACKNOWLEDGMENTS

This work is supported by Ministero dell’Istruzione, dell’Università e della Ricerca (MIUR) via the project PRIN 2017 “Taming Complexity via Quantum Strategies: A Hybrid Integrated Photonic Approach” (QUSHIP), Project No. 2017SRNBRK; by the Ministero dell’Istruzione dell’Università e della Ricerca (Ministry of Education, University and Research) program “Dipartimento di Eccellenza” (CUP:B81I18001170001); by the European Union’s Horizon 2020 research and innovation program under PHOQUSING Project GA No. 899544; and by ERC project “Composite Integrated Photonic Platform by Ultrafast Laser Micromachining” (CAPABLE), Grant Agreement No. 742745. N.S. acknowledges funding from Sapienza Università via Bando Ricerca 2018: Progetti di Ricerca Piccoli, project “Multiphase Estimation in Multiarm Interferometers.” The integrated circuit

was partially fabricated at PoliFAB, the micro- and nanofabrication facility of Politecnico di Milano [94]. F.C. and R.O.

wish to thank the PoliFAB staff for the valuable technical support.

-
- [1] V. Giovannetti, S. Lloyd, and L. Maccone, Quantum-enhanced measurements: Beating the standard quantum limit, *Science* **306**, 1330 (2004).
- [2] V. Giovannetti, S. Lloyd, and L. Maccone, Quantum Metrology, *Phys. Rev. Lett.* **96**, 010401 (2006).
- [3] V. Giovannetti, S. Lloyd, and L. Maccone, Advances in quantum metrology, *Nat. Photonics* **5**, 222 (2011).
- [4] L. Pezzé and A. Smerzi, Entanglement, Nonlinear Dynamics, and the Heisenberg Limit, *Phys. Rev. Lett.* **102**, 100401 (2009).
- [5] S. Pirandola, B. R. Bardhan, T. Gehring, C. Weedbrook, and S. Lloyd, Advances in photonic quantum sensing, *Nat. Photonics* **12**, 724 (2018).
- [6] E. Polino, M. Valeri, N. Spagnolo, and F. Sciarrino, Photonic quantum metrology, *AVS Quantum Sci.* **2**, 024703 (2020).
- [7] M. Barbieri, Optical quantum metrology, *PRX Quantum* **3**, 010202 (2022).
- [8] Z. Hou, Z. Zhang, G. Y. Xiang, C. F. Li, G. C. Guo, H. Chen, L. Liu, and H. Yuan, Minimal Tradeoff and Ultimate Precision Limit of Multiparameter Quantum Magnetometry under the Parallel Scheme, *Phys. Rev. Lett.* **125**, 020501 (2020).
- [9] L. Pezzè and A. Smerzi, Heisenberg-Limited Noisy Atomic Clock Using a Hybrid Coherent and Squeezed State Protocol, *Phys. Rev. Lett.* **125**, 210503 (2020).
- [10] S.-R. Zhao, Y.-Z. Zhang, W.-Z. Liu, J.-Y. Guan, W. Zhang, C.-L. Li, B. Bai, M.-H. Li, Y. Liu, L. You, J. Zhang, J. Fan, F. Xu, Q. Zhang, and J.-W. Pan, Field Demonstration of Distributed Quantum Sensing without Post-Selection, *Phys. Rev. X* **11**, 031009 (2021).
- [11] T. J. Proctor, P. A. Knott, and J. A. Dunningham, Multiparameter Estimation in Networked Quantum Sensors, *Phys. Rev. Lett.* **120**, 080501 (2018).
- [12] L.-Z. Liu, Y.-Z. Zhang, Z.-D. Li, R. Zhang, X.-F. Yin, Y.-Y. Fei, L. Li, N.-L. Liu, F. Xu, Y.-A. Chen, and J.-W. Pan, Distributed quantum phase estimation with entangled photons, *Nat. Photonics* **15**, 137 (2021).
- [13] X. Guo, C. R. Breum, J. Borregaard, S. Izumi, M. V. Larsen, T. Gehring, M. Christandl, J. S. Neergaard-Nielsen, and U. L. Andersen, Distributed quantum sensing in a continuous-variable entangled network, *Nat. Phys.* **16**, 281 (2020).
- [14] W. Ge, K. Jacobs, Z. Eldredge, A. V. Gorshkov, and M. Foss-Feig, Distributed Quantum Metrology with Linear Networks and Separable Inputs, *Phys. Rev. Lett.* **121**, 043604 (2018).
- [15] M. Szczykulska, T. Baumgratz, and A. Datta, Multi-parameter quantum metrology, *Adv. Phys.: X* **1**, 621 (2016).
- [16] F. Albarelli, M. Barbieri, M. G. Genoni, and I. Gianani, A perspective on multiparameter quantum metrology: From theoretical tools to applications in quantum imaging, *Phys. Lett. A* **384**, 126311 (2020).
- [17] J. Liu, H. Yuan, X.-M. Lu, and X. Wang, Quantum Fisher information matrix and multiparameter estimation, *J. Phys. A: Math. Theor.* **53**, 023001 (2020).
- [18] M. G. Paris, Quantum estimation for quantum technology, *Int. J. Quantum Inf.* **07**, 125 (2009).
- [19] R. Demkowicz-Dobrzański, W. Górecki, and M. Guţă, Multi-parameter estimation beyond quantum Fisher information, *J. Phys. A: Math. Theor.* **53**, 363001 (2020).
- [20] S. E. D'Aurelio, M. Valeri, E. Polino, V. Cimini, I. Gianani, M. Barbieri, G. Corrielli, A. Crespi, R. Osellame, F. Sciarrino, and N. Spagnolo, Experimental investigation of Bayesian bounds in multiparameter estimation, *Quantum Sci. Technol.* **7**, 025011 (2022).
- [21] J. Rubio and J. Dunningham, Bayesian multi-parameter quantum metrology with limited data, *Phys. Rev. A* **101**, 032114 (2020).
- [22] V. Cimini, M. G. Genoni, I. Gianani, N. Spagnolo, F. Sciarrino, and M. Barbieri, Diagnosing Imperfections in Quantum Sensors via Generalized Cramér-Rao Bounds, *Phys. Rev. Appl.* **13**, 024048 (2020).
- [23] H. M. Wiseman, Adaptive Phase Measurements of Optical Modes: Going Beyond the Marginal Q Distribution, *Phys. Rev. Lett.* **75**, 4587 (1995).
- [24] M. A. Ciampini, N. Spagnolo, C. Vitelli, L. Pezzè, A. Smerzi, and F. Sciarrino, Quantum-enhanced multiparameter estimation in multiarm interferometers, *Sci. Rep.* **6**, 28881 (2016).
- [25] P. C. Humphreys, M. Barbieri, A. Datta, and I. A. Walmsley, Quantum Enhanced Multiple Phase Estimation, *Phys. Rev. Lett.* **111**, 070403 (2013).
- [26] E. Polino, M. Riva, M. Valeri, R. Silvestri, G. Corrielli, A. Crespi, N. Spagnolo, R. Osellame, and F. Sciarrino, Experimental multiphase estimation on a chip, *Optica* **6**, 288 (2019).
- [27] L. Pezzè, M. A. Ciampini, N. Spagnolo, P. C. Humphreys, A. Datta, I. A. Walmsley, M. Barbieri, F. Sciarrino, and A. Smerzi, Optimal Measurements for Simultaneous Quantum Estimation of Multiple Phases, *Phys. Rev. Lett.* **119**, 130504 (2017).
- [28] S. Hong, J. ur Rehman, Y.-S. Kim, Y.-W. Cho, S.-W. Lee, H. Jung, S. Moon, S.-W. Han, and H.-T. Lim, Quantum enhanced multiple-phase estimation with multi-mode $N00N$ states, *Nat. Commun.* **12**, 5211 (2021).
- [29] J. Carolan, C. Harrold, C. Sparrow, E. Martín-López, N. J. Russell, J. W. Silverstone, P. J. Shadbolt, N. Matsuda, M. Oguma, M. Itoh, G. D. Marshall, M. G. Thompson, J. C. F. Matthews, T. Hashimoto, J. L. O'Brien, and A. Laing, Universal linear optics, *Science* **349**, 711 (2015).
- [30] J. Wang, F. Sciarrino, A. Laing, and M. G. Thompson, Integrated photonic quantum technologies, *Nat. Photonics* **14**, 273 (2020).
- [31] G. Corrielli, A. Crespi, and R. Osellame, Femtosecond laser micromachining for integrated quantum photonics, *Nanophotonics* **10**, 3789 (2021).
- [32] M. Valeri, E. Polino, D. Poderini, I. Gianani, G. Corrielli, A. Crespi, R. Osellame, N. Spagnolo, and F. Sciarrino, Experimental adaptive Bayesian estimation of multiple phases with limited data, *npj Quantum Inf.* **6**, 92 (2020).
- [33] G.-Y. Xiang, B. L. Higgins, D. Berry, H. M. Wiseman, and G. Pryde, Entanglement-enhanced measurement of a completely unknown optical phase, *Nat. Photonics* **5**, 43 (2011).

- [34] A. A. Berni, A. A. Berni, T. Gehring, B. M. Nielsen, V. Händchen, M. G. A. Paris, and U. L. Andersen, *Ab initio* quantum-enhanced optical phase estimation using real-time feedback control, *Nat. Photonics* **9**, 577 (2015).
- [35] S. Daryanoosh, S. Slussarenko, D. W. Berry, H. M. Wiseman, and G. J. Pryde, Experimental optical phase measurement approaching the exact Heisenberg limit, *Nat. Commun.* **9**, 4606 (2018).
- [36] T. Baumgratz and A. Datta, Quantum Enhanced Estimation of a Multidimensional Field, *Phys. Rev. Lett.* **116**, 030801 (2016).
- [37] W. Górecki and R. Demkowicz-Dobrzański, Multiple-Phase Quantum Interferometry: Real and Apparent Gains of Measuring All the Phases Simultaneously, *Phys. Rev. Lett.* **128**, 040504 (2022).
- [38] W. Górecki and R. Demkowicz-Dobrzański, Multiparameter quantum metrology in the Heisenberg limit regime: Many-repetition scenario versus full optimization, *Phys. Rev. A* **106**, 012424 (2022).
- [39] M. D. Vidrighin, G. Donati, M. G. Genoni, X.-M. Jin, W. S. Kolthammer, M. S. Kim, A. Datta, M. Barbieri, and I. A. Walmsley, Joint estimation of phase and phase diffusion for quantum metrology, *Nat. Commun.* **5**, 3532 (2014).
- [40] E. Roccia, V. Cimini, M. Sbroscia, I. Gianani, L. Ruggiero, L. Mancino, M. G. Genoni, M. A. Ricci, and M. Barbieri, Multiparameter approach to quantum phase estimation with limited visibility, *Optica* **5**, 1171 (2018).
- [41] C. W. Helstrom, *Quantum Detection and Estimation Theory* (Academic, New York, 1976).
- [42] S. Ragy, M. Jarzyna, and R. Demkowicz-Dobrzański, Compatibility in multiparameter quantum metrology, *Phys. Rev. A* **94**, 052108 (2016).
- [43] A. Z. Goldberg, L. L. Sánchez-Soto, and H. Ferretti, Intrinsic Sensitivity Limits for Multiparameter Quantum Metrology, *Phys. Rev. Lett.* **127**, 110501 (2021).
- [44] Y. Li, L. Pezzè, M. Gessner, Z. Ren, W. Li, and A. Smerzi, Frequentist and Bayesian quantum phase estimation, *Entropy* **20**, 628 (2018).
- [45] M. Malitesta, A. Smerzi, and L. Pezzè, Distributed quantum sensing with squeezed-vacuum light in a configurable network of Mach-Zehnder interferometers, [arXiv:2109.09178](https://arxiv.org/abs/2109.09178).
- [46] K. K. Lee, C. N. Gagatsos, S. Guha, and A. Ashok, Quantum-inspired multi-parameter adaptive Bayesian estimation for sensing and imaging, *IEEE J. Sel. Top. Signal Process.* (2022), doi: [10.1109/JSTSP.2022.3214774](https://doi.org/10.1109/JSTSP.2022.3214774).
- [47] V. Cimini, M. Mellini, G. Rampioni, M. Sbroscia, L. Leoni, M. Barbieri, and I. Gianani, Adaptive tracking of enzymatic reactions with quantum light, *Opt. Express* **27**, 35245 (2019).
- [48] B. L. Higgins, D. W. Berry, S. D. Bartlett, H. M. Wiseman, and G. J. Pryde, Entanglement-free Heisenberg-limited phase estimation, *Nature (London)* **450**, 393 (2007).
- [49] A. Lumino, E. Polino, A. S. Rab, G. Milani, N. Spagnolo, N. Wiebe, and F. Sciarrino, Experimental Phase Estimation Enhanced by Machine Learning, *Phys. Rev. Appl.* **10**, 044033 (2018).
- [50] C. E. Granade, C. Ferrie, N. Wiebe, and D. G. Cory, Robust online Hamiltonian learning, *New J. Phys.* **14**, 103013 (2012).
- [51] V. Gebhart, A. Smerzi, and L. Pezzè, Bayesian Quantum Multiphase Estimation Algorithm, *Phys. Rev. Appl.* **16**, 014035 (2021).
- [52] V. Cimini, M. Valeri, E. Polino, S. Piacentini, F. Ceccarelli, G. Corrielli, N. Spagnolo, R. Osellame, and F. Sciarrino, Deep reinforcement learning for quantum multiparameter estimation, [arXiv:2209.00671](https://arxiv.org/abs/2209.00671).
- [53] C. Macchiavello, Optimal estimation of multiple phases, *Phys. Rev. A* **67**, 062302 (2003).
- [54] J. Liu, X.-M. Lu, Z. Sun, and X. Wang, Quantum multiparameter metrology with generalized entangled coherent state, *J. Phys. A: Math. Theor.* **49**, 115302 (2016).
- [55] C. N. Gagatsos, D. Branford, and A. Datta, Gaussian systems for quantum-enhanced multiple phase estimation, *Phys. Rev. A* **94**, 042342 (2016).
- [56] M. Gessner, L. Pezzè, and A. Smerzi, Sensitivity Bounds for Multiparameter Quantum Metrology, *Phys. Rev. Lett.* **121**, 130503 (2018).
- [57] C. Oh, C. Lee, S. H. Lie, and H. Jeong, Optimal distributed quantum sensing using Gaussian states, *Phys. Rev. Res.* **2**, 023030 (2020).
- [58] A. Z. Goldberg, I. Gianani, M. Barbieri, F. Sciarrino, A. M. Steinberg, and N. Spagnolo, Multiphase estimation without a reference mode, *Phys. Rev. A* **102**, 022230 (2020).
- [59] M. A. Taylor, J. Janousek, V. Daria, J. Knittel, B. Hage, H.-A. Bachor, and W. P. Bowen, Biological measurement beyond the quantum limit, *Nat. Photonics* **7**, 229 (2013).
- [60] P.-A. Moreau, E. Toninelli, T. Gregory, and M. J. Padgett, Imaging with quantum states of light, *Nat. Rev. Phys.* **1**, 367 (2019).
- [61] M. A. Taylor and W. P. Bowen, Quantum metrology and its application in biology, *Phys. Rep.* **615**, 1 (2016).
- [62] S. Mukamel, M. Freyberger, W. Schleich, M. Bellini, A. Zavatta, G. Leuchs, C. Silberhorn, R. W. Boyd, L. L. Sánchez-Soto, A. Stefanov, M. Barbieri, A. Paterova, L. Krivitsky, S. Shwartz, K. Tamasaku, K. Dorfman, F. Schlawin, V. Sandoghdar, M. Raymer, A. Marcus *et al.*, Roadmap on quantum light spectroscopy, *J. Phys. B: At., Mol. Opt. Phys.* **53**, 072002 (2020).
- [63] T. Rudolph and L. Grover, Quantum Communication Complexity of Establishing a Shared Reference Frame, *Phys. Rev. Lett.* **91**, 217905 (2003).
- [64] P. J. O'Malley, R. Babbush, I. D. Kivlichan, J. Romero, J. R. McClean, R. Barends, J. Kelly, P. Roushan, A. Tranter, N. Ding, B. Campbell, Y. Chen, Z. Chen, B. Chiaro, A. Dunsworth, A. G. Fowler, E. Jeffrey, E. Lucero, A. Megrant, J. Y. Mutus *et al.*, Scalable Quantum Simulation of Molecular Energies, *Phys. Rev. X* **6**, 031007 (2016).
- [65] The LIGO Scientific Collaboration, A gravitational wave observatory operating beyond the quantum shot-noise limit, *Nat. Phys.* **7**, 962 (2011).
- [66] T. Meany, M. Gräfe, R. Heilmann, A. Perez-Leija, S. Gross, M. J. Steel, M. J. Withford, and A. Szameit, Laser written circuits for quantum photonics, *Laser Photonics Rev.* **9**, 363 (2015).
- [67] M. Żukowski, A. Zeilinger, and M. A. Horne, Realizable higher-dimensional two-particle entanglements via multipoint beam splitters, *Phys. Rev. A* **55**, 2564 (1997).
- [68] F. Ceccarelli, S. Atzeni, C. Pentangelo, F. Pellegatta, A. Crespi, and R. Osellame, Low power reconfigurability and reduced crosstalk in integrated photonic circuits fabricated by femtosecond laser micromachining, *Laser Photonics Rev.* **14**, 2000024 (2020).

- [69] See Supplemental Material at <http://link.aps.org/supplemental/10.1103/PhysRevResearch.5.013138> for details regarding the circuit geometry, the waveguide inscription, the thermal shifter fabrication processes, the thermal shifter performance, the use of completely distinguishable photons, the calibration procedure, the Bayesian framework, and the sequential Monte Carlo technique, as well as a table of the state-of-the-art results.
- [70] L. Pezzé and A. Smerzi, Mach-Zehnder Interferometry at the Heisenberg Limit with Coherent and Squeezed-Vacuum Light, *Phys. Rev. Lett.* **100**, 073601 (2008).
- [71] F. Vernuccio, A. Bresci, V. Cimini, A. Giuseppi, G. Cerullo, D. Polli, and C. M. Valensise, Artificial intelligence in classical and quantum photonics, *Laser Photonics Rev.* **16**, 2100399 (2022).
- [72] S. Nolan, A. Smerzi, and L. Pezzè, A machine learning approach to Bayesian parameter estimation, *npj Quantum Inf.* **7**, 169 (2021).
- [73] L. J. Fiderer, J. Schuff, and D. Braun, Neural-network heuristics for adaptive bayesian quantum estimation, *PRX Quantum* **2**, 020303 (2021).
- [74] V. Cimini, I. Gianani, N. Spagnolo, F. Leccese, F. Sciarrino, and M. Barbieri, Calibration of Quantum Sensors by Neural Networks, *Phys. Rev. Lett.* **123**, 230502 (2019).
- [75] V. Cimini, E. Polino, M. Valeri, I. Gianani, N. Spagnolo, G. Corrielli, A. Crespi, R. Osellame, M. Barbieri, and F. Sciarrino, Calibration of Multiparameter Sensors via Machine Learning at the Single-Photon Level, *Phys. Rev. Appl.* **15**, 044003 (2021).
- [76] T. Xiao, J. Fan, and G. Zeng, Parameter estimation in quantum sensing based on deep reinforcement learning, *npj Quantum Inf.* **8**, 2 (2022).
- [77] N. Wiebe and C. E. Granade, Efficient Bayesian Phase Estimation, *Phys. Rev. Lett.* **117**, 010503 (2016).
- [78] A. Crespi, M. Lobino, J. C. F. Matthews, A. Politi, C. R. Neal, R. Ramponi, R. Osellame, and J. L. O'Brien, Measuring protein concentration with entangled photons, *Appl. Phys. Lett.* **100**, 233704 (2012).
- [79] O. Varnavski, C. Gunthardt, A. Rehman, G. D. Luker, and T. Goodson III, Quantum light-enhanced two-photon imaging of breast cancer cells, *J. Phys. Chem. Lett.* **13**, 2772 (2022).
- [80] F. Wolfgramm, C. Vitelli, F. A. Beduini, N. Godbout, and M. W. Mitchell, Entanglement-enhanced probing of a delicate material system, *Nat. Photonics* **7**, 28 (2013).
- [81] R. Tenne, U. Rossman, B. Rephael, Y. Israel, A. Krupinski-Ptaszek, R. Lapkiewicz, Y. Silberberg, and D. Oron, Super-resolution enhancement by quantum image scanning microscopy, *Nat. Photonics* **13**, 116 (2019).
- [82] J.-P. Chen, C. Zhang, Y. Liu, C. Jiang, D.-F. Zhao, W.-J. Zhang, F.-X. Chen, H. Li, L.-X. You, Z. Wang, Y. Chen, X.-B. Wang, Q. Zhang, and J.-W. Pan, Quantum Key Distribution over 658 km Fiber with Distributed Vibration Sensing, *Phys. Rev. Lett.* **128**, 180502 (2022).
- [83] Y. Xia, W. Li, W. Clark, D. Hart, Q. Zhuang, and Z. Zhang, Demonstration of a Reconfigurable Entangled Radio-Frequency Photonic Sensor Network, *Phys. Rev. Lett.* **124**, 150502 (2020).
- [84] P. Kómár, E. M. Kessler, M. Bishof, L. Jiang, A. S. Sørensen, J. Ye, and M. D. Lukin, A quantum network of clocks, *Nat. Phys.* **10**, 582 (2014).
- [85] A. Aspuru-Guzik, A. D. Dutoi, P. J. Love, and M. Head-Gordon, Simulated quantum computation of molecular energies, *Science* **309**, 1704 (2005).
- [86] S. McArdle, S. Endo, A. Aspuru-Guzik, S. C. Benjamin, and X. Yuan, Quantum computational chemistry, *Rev. Mod. Phys.* **92**, 015003 (2020).
- [87] V. Cimini, E. Polino, F. Belliardo, F. Hoch, B. Piccirillo, N. Spagnolo, V. Giovannetti, and F. Sciarrino, Non-asymptotic Heisenberg scaling: experimental metrology for a wide resources range, [arXiv:2110.02908](https://arxiv.org/abs/2110.02908).
- [88] S. Yokoyama, R. Ukai, S. C. Armstrong, C. Sornphiphatphong, T. Kaji, S. Suzuki, J.-i. Yoshikawa, H. Yonezawa, N. C. Menicucci, and A. Furusawa, Ultra-large-scale continuous-variable cluster states multiplexed in the time domain, *Nat. Photonics* **7**, 982 (2013).
- [89] E. Moreau, I. Robert, J. M. Gérard, I. Abram, L. Manin, and V. Thierry-Mieg, Single-mode solid-state single photon source based on isolated quantum dots in pillar microcavities, *Appl. Phys. Lett.* **79**, 2865 (2001).
- [90] S. Slussarenko, M. M. Weston, H. M. Chrzanowski, L. K. Shalm, V. B. Verma, S. W. Nam, and G. J. Pryde, Unconditional violation of the shot-noise limit in photonic quantum metrology, *Nat. Photonics* **11**, 700 (2017).
- [91] S. Atzeni, A. S. Rab, G. Corrielli, E. Polino, M. Valeri, P. Mataloni, N. Spagnolo, A. Crespi, F. Sciarrino, and R. Osellame, Integrated sources of entangled photons at the telecom wavelength in femtosecond-laser-written circuits, *Optica* **5**, 311 (2018).
- [92] S. Paesani, M. Borghi, S. Signorini, A. Mañnos, L. Pavesi, and A. Laing, Near-ideal spontaneous photon sources in silicon quantum photonics, *Nat. Commun.* **11**, 2505 (2020).
- [93] J. Chang, J. W. N. Los, J. O. Tenorio-Pearl, N. Noordzij, R. Gourgues, A. Guardiani, J. R. Zichi, S. F. Pereira, H. P. Urbach, V. Zwiller, S. N. Dorenbos, and I. E. Zadeh, Detecting telecom single photons with $(99.5^{+0.5}_{-2.07})\%$ system detection efficiency and high time resolution, *APL Photonics* **6**, 036114 (2021).
- [94] <https://www.polifab.polimi.it/>.